Fast 4D Segmentation of Large Datasets using Graph Cuts

Herve Lombaert[a], Yiyong Sun[b], and Farida Cheriet[a]

[a]École Polytechnique de Montréal, Montréal, Québec, Canada
[b]Siemens Corporate Research, Princeton, NJ 08540, USA

ABSTRACT

In this paper, we propose to use 4D graph cuts for the segmentation of large spatio-temporal (4D) datasets. Indeed, as 4D datasets grow in popularity in many clinical areas, so will the demand for efficient general segmentation algorithms. The graph cuts method[1] has become a leading method for complex 2D and 3D image segmentation in many applications. Despite a few attempts[2–5] in 4D, the use of graph cuts on typical medical volume quickly exceeds today's computer capacities. Among all existing graph cuts based methods[6–10] the multilevel banded graph cuts[9] is the fastest and uses the least amount of memory. Nevertheless, this method has its limitation. Memory becomes an issue when using large 4D volume sequences, and small structures become hardly recoverable when using narrow bands. We thus improve the boundary refinement efficiency by using a 4D competitive region growing. First, we construct a coarse graph at a low resolution with strong temporal links to prevent the shrink bias inherent to the graph cuts method. Second, we use a competitive region growing using a priority queue to capture all fine details. Leaks are prevented by constraining the competitive region growing within a banded region and by adding a viscosity term. This strategy yields results comparable to the multilevel banded graph cuts but is faster and allows its application to large 4D datasets. We applied our method on both cardiac 4D MRI and 4D CT datasets with promising results.

1. INTRODUCTION

The amount of information contained in medical images can become overwhelming during an intervention, especially when dealing with volume sequences. The time spent in interpreting these images can be greatly decreased with segmentation algorithms, highlighting anatomical structures of interest, thus leading to a better image understanding and organ localization. Spatial images (2D and 3D) have been heavily studied. Spatio-temporal images (4D, or 3D+t) are becoming widely available and they still present an unsolved computational challenge. Scanners output gigabytes of data and the trend is towards even higher definitions.

Explicit deformable models[11,12] have been used as initial attempts for 4D segmentation. Free form deformations[11] and simplex meshes[12] have been applied in the temporal domain to track 3D surfaces over time. However, 4D segmentation is not treated as a whole; the temporal dimension is rather treated separately. The surface of a particular frame serves as an initial guess for the next frame. Later, temporal correlation[13] is considered by adding 4D *a priori* knowledge in the segmentation. A probabilistic 4D atlas[14] can help the segmentation using the EM algorithm, and temporal constraints[15] can also be incorporated in a 4D deformable model. The level set method[16] is a well established segmentation algorithm in 2D and 3D images. Although this method is easily extendable to N-D, few works have been done in 4D. For instance, a 4D levelset[17] is used to approximate the aortic shape, the surface itself is computed with a graph-based method. Shape priors are used[18,19] to improve the segmentation of low quality images. The Graph Cuts method[20] uses the maxflow algorithm to find the minimum cut on a graph. Compared with the previous local approaches, maxflow-mincut algorithms yield optimal solutions in polynomial time. Graph Cuts have already been used for 4D surface selection[2] and reconstruction.[21] In image segmentation, although being N-D interactive, Boykov and Jolly's method[1] is impractical for typical 4D medical datasets using current processing capacities. New designs have been proposed to get around this issue. Active contours[6] are simulated by evolving banded graph cuts. However, in this method, the band inner boundary has a smaller surface than the band outer boundary; the difference in surface area creates a shrinkage bias. Lazy snapping[7,22] uses the graph cuts technique on watershed regions of the image. The algorithm pre-segmentation is however time consuming when using large datasets, and produces an unpredictable number of watershed regions. Moreover, the fine segmentation depends on the watershed boundaries, and as shown in,[23] these boundaries are not necessarily robust to noise. Rather than watershed regions, the mean shift algorithm

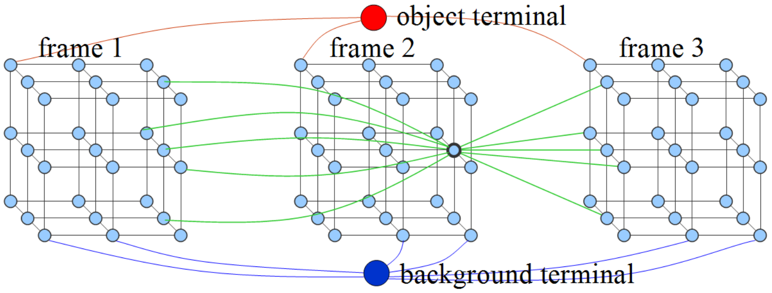

Figure 1. 4D graph corresponding to 3 frames of a 3^3 volume. Spatial *n-links* in grey lines, temporal *n-links* for a single node in green lines, and *t-links* in red and blue.

has been used[8] to segment objects in a (2D+t) video. This method still relies on pre-segmented results, which are also time-consuming in this case. A different coarse-to-fine approach is the multilevel banded graph cuts method.[9] The algorithm iteratively projects the results from a coarse image up to the fine resolution. Results in 2D and 3D are comparable to the standard graph cut algorithm. However, small and thin structures can easily be lost with this method when using very large 4D datasets. Active Graph Cuts[10] could solve this problem as it retains the global optimality of the solution, but requires the same amount of memory than the standard graph cuts. Laplacian pyramids[24] could be used in order to catch finer details. These graph cuts based techniques are all efficient with 2D and 3D images, but the memory required by large 4D datasets is prohibitive.

We propose in section 2 a segmentation method based on 4D graph cuts. To overcome the computational limitation, a coarse-to-fine strategy is developed. Results presented in section 3 show that the segmentation accuracy is indeed improved when using 4D graph cuts rather than when using 3D graph cuts sequentially. Moreover, our method performs well in segmentation of cardiac structures on both 4D MR and 4D CT. A general discussion as well as guidelines for future work are provided in section 4.

2. METHOD

First, the graph cuts algorithm for image segmentation[20] is briefly described. In a graph representing a 4D image, a cut separates graph nodes into two categories, object and background. Second,a coarse-to-fine strategy is developed in order to successfully run the method on large 4D datasets.

2.1 4D Graph Cuts

Given a 4D image, a weighted undirected graph $\mathcal{G} = \langle \mathcal{V}, \mathcal{E} \rangle$ is constructed (Fig. 1). There are two special nodes, or vertices, in $\mathcal{V}$, a source node specifying the "object" terminal, and a sink node specifying the "background" terminal. Each remaining node in $\mathcal{V}$ uniquely identifies an image point. There are two types of edges in $\mathcal{E}$, *n-links* (spatial and temporal neighborhood links), and *t-links* (terminal links). Each image node has two *t-links* connecting the node to the terminals. The *n-links* are determined by a spatio-temporal neighborhood system $\mathcal{N}$, e.g., $|\mathcal{N}^{(t)}| = 26$ and $|\mathcal{N}^{(t-1)}| = |\mathcal{N}^{(t+1)}| = 6$. The weight used for edges between two nodes p and q is based on the data intensity difference. Boykov and Jolly[1] proposed to use the weight for spatial *n-links* as $w_{p,q} = f(|I_p - I_q|)$ with $f(x) = e^{-\frac{x^2}{\sigma^2}}$ where σ is a smoothness parameter. We define the weight of temporal *n-links* as $w_{p^{(t)},q^{(t+1)}} = \tau \cdot f(|I_{p^{(t)}} - I_{q^{(t+1)}}|)$, where τ is a parameter implementing temporal integrity. Additionally, the user provides the seed points $\mathcal{O}$ and $\mathcal{B}$ marked as "object" and "background" (Fig. 2(a)). The *t-links* of these seed points have infinity weights, i.e., $w_{p,\text{"obj"}} = \infty | p \in \mathcal{O}$, and $w_{p,\text{"bkg"}} = \infty | p \in \mathcal{B}$. Zero weight *t-links* are used elsewhere. The segmentation is determined by a cut $\mathcal{C}$ on the graph. Severed edges in $\mathcal{E}$ separate the terminal nodes, classifying each image node into either object or background. The cost of a cut is the sum of all severed edges: $|\mathcal{C}| = \sum_{e_{p,q} \in \mathcal{C}} w_{p,q}$. Therefore, segmentation can be solved by finding the minimum cut on the graph. This can be computed efficiently with polynomial-time complexity algorithms such as Boykov and Kolmogorov's maxflow implementation.[20]

The graph cuts method is known[25] to have a bias towards small cuts. The cost of a small cut surrounding the seed points might be cheaper than the cost of a larger cut around the object's boundary. In 4D, it might

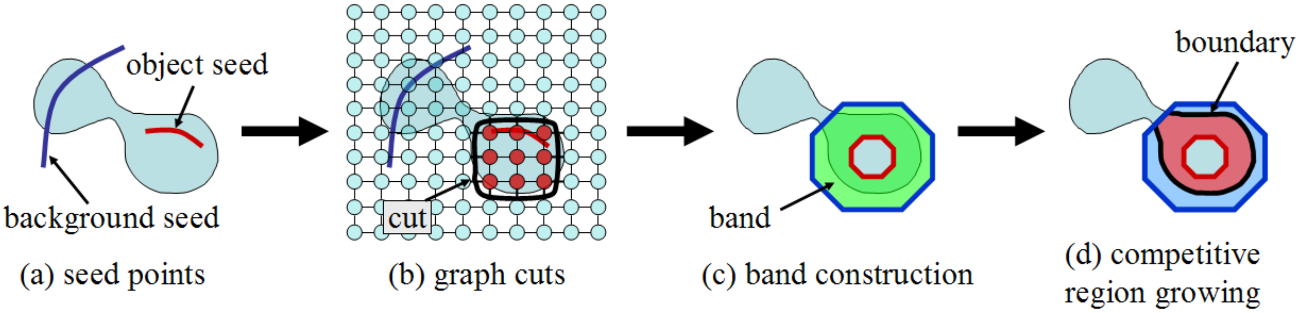

Figure 2. Banded approach: (a) object and background seed points provided by the user; (b) global shape computed via graph cuts; (c) construction of the band around the coarse boundary; (d) refinement of the boundary (thick black contour) using fast competitive region growing.

be cheaper to segment the organ in a single 3D frame rather than in the whole 4D sequence. We propose to use slightly more expensive temporal *n-links*. When the object is assumed to be seen on all frames, stronger temporal correlation are imposed with $\tau > 1$.

2.2 Fast Banded Approach

For typical medical datasets, a 4D graph needs a prohibitive amount of memory. For example, the maxflow implementation from Boykov and Kolmogorov[20] requires $24|\mathcal{V}| + 14|\mathcal{E}|$ bytes. That is over 21GB for a 4D 10×256^3 dataset. Furthermore, the polynomial complexity of the algorithm makes graph cuts impractical using today's processing power. To overcome this problem, the graph is constructed at a low resolution. The 4D data is scaled down by a factor k using the mean filter, so the resulting graph fits in the computer's memory. Similarly, the seed point coordinates are scaled down by the factor k. Note that this factor can be different for each dimension (e.g., $k > 1$ for spatial dimensions and $k = 1$ for the temporal dimension).

The segmentation resulting from the low resolution graph is refined in a band around the graph's minimum cut (Fig. 2(c)). The band radius is ideally the size of one low resolution voxel, or k voxels in high resolution. It is assumed that the inner surface of the band remains inside the object, and that the outer band remains outside it. The boundary is refined using competitive region growing between the inner and the outer surfaces within the band. Leaking, inherent to region growing algorithms, is thus confined in the band. Note that the boundary refinement takes place in 4D, a hyper-band and hyper-regions are indeed used. Similarly to the seeded region growing,[23] all potentially new object or background voxels are placed in one priority queue. Their order in the queue depends on the intensity difference $\mathit{diff}(p) = |I_p - I_{par(p)}|$ between the candidate voxel p and its parent $par(p)$. For a newly inserted voxel in the priority queue, its key value $key(p)$ is an integration of previous keys, i.e., $key(p) = \mathit{diff}(p) + \lambda \cdot key(par(p))$, with λ bounded between 0 and 1. Regions first grow to include voxels with similar intensities. However, when $\lambda > 0$, this heuristics favors the growing of regions close to the seed points. Hence, λ simulates the smoothness of the grown boundary. In the section 3.2, a comparison between the multilevel banded graph cuts[9] and this competitive region growing shows that both methods yield comparable results.

Optionally, the refinement step can be iterative. During an iteration, a new band is constructed around the previous refined boundary. This band evolution allows an incremental segmentation of structures not fully present in the initial band (e.g., vessels originating, or ending, in the segmented organ). However, as the competitive region growing does not yield a global optimum result, there is no guarantee of convergence to such an iterative approach.

3. RESULTS

The method is compared with the standard graph cuts. The results, although slightly different, show that this new method is a valid alternative when using very large 4D datasets. Segmentations of cardiac structures on both 4D MR and 4D CT are presented.

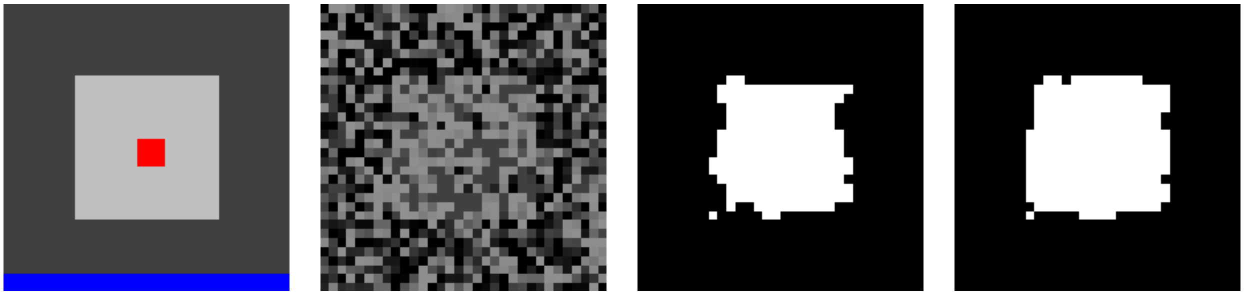

(a) ground truth (b) noisy image (c) 3D slice (d) 4D slice

Figure 3. 4D vs. 3D Segmentation with Graph Cuts: (a) ground truth with seed points, (b) image with noise, (c) slice from the 3D segmentation (12.89% error with the ground truth), (d) slice from the 4D segmentation (7.35% error with the ground truth).

3.1 4D vs. 3D Segmentation with Graph Cuts

Temporal correlations improves the segmentation accuracy. It is demonstrated with a noisy synthetic image where a ground truth is known. The segmentation accuracy is compared when using the algorithm in a 3D version and in a 4D version. The 4D volume (5×32^3) has a static bright cube of intensity 0.75 on a dark background of intensity 0.25 (Fig. 3(a)). A Gaussian noise with $\sigma = 0.35$ is added to the image. With such a strong noise, spatial information becomes weak (Fig. 3(b)). A 3D segmentation of a single 3D frame yields 12.89% of error compared to the ground truth; 0.59% of the voxels are over-segmented, and 12.30% are under-segmented (Fig. 3(c)). When temporal information is added in a 4D graph ($|\mathcal{N}^{(t)}| = 26, |\mathcal{N}^{(t-1)}| = |\mathcal{N}^{(t+1)}| = 6$), the segmentation error drops to 7.35%; 0.98% of the voxels are over-segmented, and 6.37% of the voxels are under-segmented (Fig. 3(d)).

3.2 Fast 4D Segmentation

In order to measure the computational improvement of our method, a single frame from a $15 \times 192 \times 192 \times 80$ MR volume is used (Fig. 4(a)). With a core 2 duo 2.8GHz and 2GB of memory, the standard graph cuts runs in 20.88s, and requires 1270MB of memory (Fig. 4(b)). With one level using a downscaling factor $k = 5$, the multilevel banded graph cuts runs in 1.53s, and requires 47.5MB of memory. Our method runs in 0.59s and requires 13.6MB of memory.

When considering the whole sequence (15 frames), 23GB of memory would be required to construct a standard 4D graph. This is not possible with current computers. Since there is no ground truth available for the left ventricle segmentation, our method is compared with the multilevel banded graph cuts. The latter runs in 44.72s, and requires 854MB (Fig. 4(c)). With the same conditions, our method runs in 9.42s, and requires 253MB; 3.46% of the voxels are under-segmented, and 5.52% of the voxels are over-segmented (Fig. 4(d)). After a second iteration of the boundary refinement, the error drops to 3.62% of under-segmented and 4.45% of over-segmented

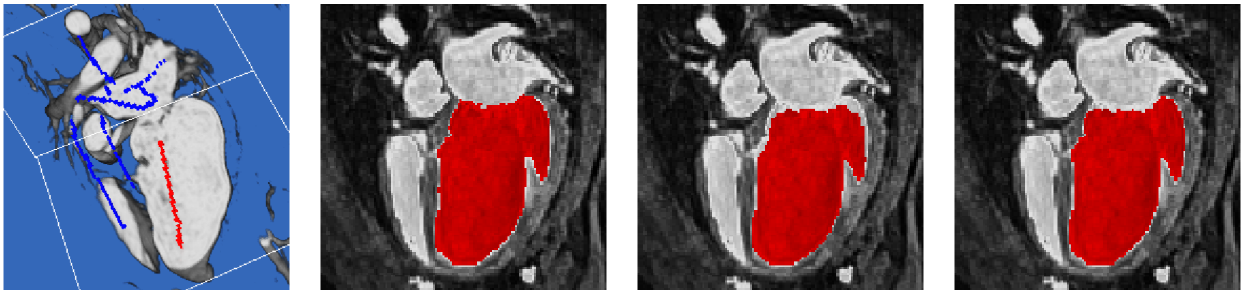

(a) seed points (b) 3D Graph Cuts (c) 4D M. banded GC (d) our method

Figure 4. Comparison with existing methods: (a) seed points for the left ventricle segmentation, (b) 3D standard graph cuts on a single frame (20.88s, 1270MB), (c) 4D multilevel banded graph cuts on 15 frames (44.72s, 854MB), (d) our method on 15 frames (9.42sec, 253MB).

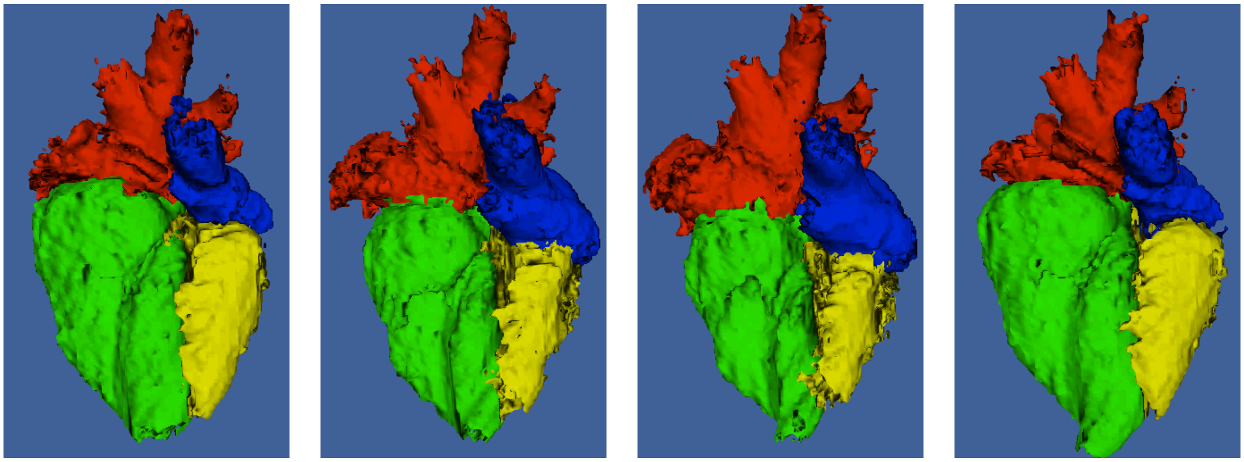

Figure 5. 4D MR Segmentation of the Left Atrium in red (10.50s, 253MB), of the Left Ventricle in green (9.51s, 253MB), of the Right Atrium in blue (9.51s, 253MB), and of the Right Ventricle in yellow (10.83s, 253MB) from a $15 \times 192 \times 192 \times 80$ data.

voxels. It is possible to see differences between the multilevel banded graph cuts and our method in regions with weak boundaries, for instance, between the left ventricle and the left atrium.

3.3 Segmentation of Cardiac Structures

From the 4D MR dataset, all 4 cardiac chambers are segmented (Fig. 5 shows the left atrium segmented in 10.50s, 253.8MB; left ventricle, 9.51s, 253.8MB; right atrium, 8.92s, 253.8MB; right ventricle, 10.83s, 253.8MB). On even larger 4D datasets, the multilevel banded graph cuts runs out of memory. Multilevels can be used at the expense of computation time. It is also possible to foresee the memory problem with very large datasets. Our method runs successfully on these large datasets. Cardiac structures of a human heart are segmented in a $10 \times 512 \times 512 \times 141$ CT sequence (Fig. 6). To segment the left atrium, 79.42s and 1367MB is required. Details of the algorithm show that the low resolution graph cuts used as little as 4.86s, and the competitive region growing runs in 21.58s. Much of the computation time is spent constructing the band (30sec) as well as scaling down and scaling up the volume (10sec each). To segment the left ventricle, 81.20s and 1371MB is required.

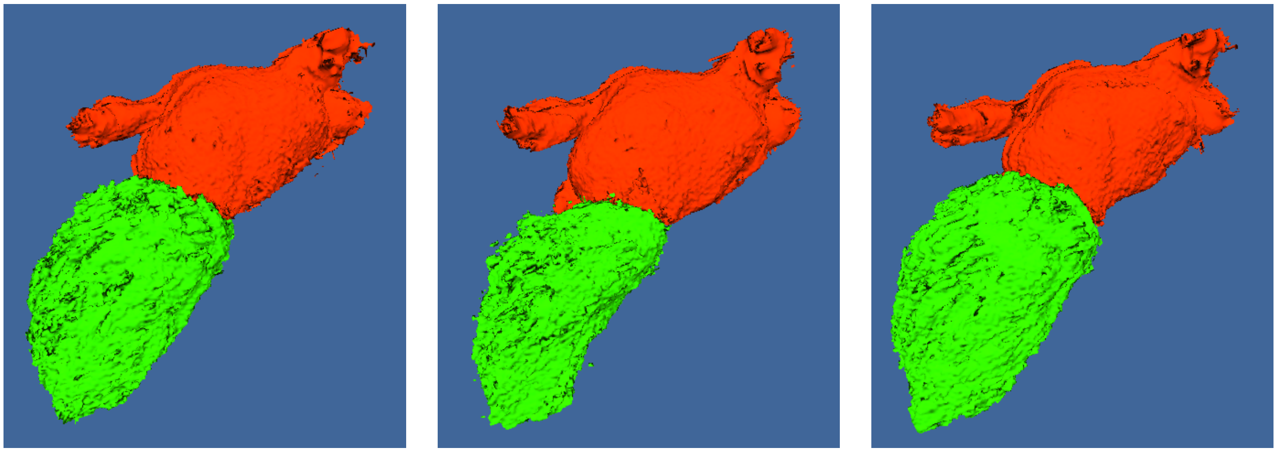

Figure 6. 4D CT Segmentation of the Left Atrium in red (79.42s, 1367MB), of the Left Ventricle in green (81.20s, 1371MB) from a $10 \times 512 \times 512 \times 141$ data.

4. CONCLUSIONS

In this paper, 4D graph cuts have been proposed for 4D segmentation. The results showed that temporal correlation improves the segmentation accuracy of very noisy data. In order to use graph cuts in typical medical volumes, a coarse-to-fine strategy has been developed. In our proposed method, which is applicable to both 3D and 4D, we improved the boundary refinement using competitive region growing. Besides yielding comparable results, our approach is faster and uses less memory than the multilevel banded graph cuts. It is therefore well suited for applications with very large 4D datasets. Our method shows promising results with the segmentation of both 4D MR and 4D CT.

Drawbacks of our method are inherent to the graph cut method. The seed size is important. If it is small, a small graph cut around the seeds can be cheaper than a larger graph cut around the organ. In 4D datasets, it might be cheaper to cut the organ within a single 3D frame rather than in all frames. This is usually solved by using large seeds. To prevent these small cuts, we propose to use heavier weights for temporal links between frames. Future work will further investigate this issue.

Acknowledgement

The authors wish to acknowledge the financial support from Siemens Corporate Research (SCR) and the Natural Sciences and Engineering Research Council of Canada (NSERC).

REFERENCES

[1] Boykov, Y. and Jolly, M.-P., "Interactive Organ Segmentation Using Graph Cuts," in [*MICCAI*], 276–286 (2000).

[2] Waschbüsch, M., Würmlin, S., and Gross, M., "Interactive 3D video editing," *Visual Computer* **22**(9), 631–641 (2006).

[3] Bai, X., Wang, J., Simons, D., and Sapiro, G., "Video snapcut: robust video object cutout using localized classifiers," in [*SIGGRAPH*], 1–11 (2009).

[4] Vaudrey, T., Gruber, D., Wedel, A., and Klappstein, J., "Space-time multi-resolution banded graph-cut for fast segmentation," in [*DAGM Symposium Pattern Recognition*], 203–213 (2008).

[5] Lombaert, H. and Cheriet, F., "Spatio-temporal segmentation of the heart in 4d mri images using graph cuts with motion cues," in [*ISBI*], (2010).

[6] Xu, N., Bansal, R., and Ahuja, N., "Object segmentation using graph cuts based active contours," in [*CVPR*], 46–53 (2003).

[7] Li, Y., Sun, J., Tang, C.-K., and Shum, H.-Y., "Lazy snapping," in [*SIGGRAPH*], 303–308 (2004).

[8] Wang, J., Bhat, P., Colburn, A. R., Agrawala, M., and Cohen, M. F., "Interactive video cutout," in [*SIGGRAPH*], 585–594 (2005).

[9] Lombaert, H., Sun, Y., Grady, L., and Xu, C., "A Multilevel Banded Graph Cuts Method for Fast Image Segmentation," in [*ICCV*], 259–265 (2005).

[10] Juan, O. and Boykov, Y., "Active Graph Cuts," in [*CVPR*], 1023–1029 (2006).

[11] Bardinet, E., Cohen, L. D., and Ayache, N., "Tracking and motion analysis of the left ventricle with deformable superquadrics.," *Medical Image Analysis* **1**(2), 129–149 (1996).

[12] McInerney, T. and Terzopoulos, D., "A dynamic finite element surface model for segmentation and tracking in multidimensional medical images with application to cardiac 4D image analysis," *Computerized Medical Imaging and Graphics* **19**(1), 69–83 (1995).

[13] Chandrashekara, R., Rao, A., Sanchez-Ortiz, G. I., Mohiaddin, R. H., and Rueckert, D., "Construction of a Statistical Model for Cardiac Motion Analysis Using Nonrigid Image Registration," in [*IPMI*], 599–610 (2003).

[14] Lorenzo-Valdés, M., Sanchez-Ortiz, G. I., Mohiaddin, R., and Rueckert, D., "Segmentation of 4D Cardiac MR Images Using a Probabilistic Atlas and the EM Algorithm," in [*MICCAI*], 440–450 (2003).

[15] Montagnat, J. and Delingette, H., "4D deformable models with temporal constraints: application to 4D cardiac image segmentation.," *Medical Image Analysis* **9**(1), 87–100 (2005).

[16] Osher, S. and Sethian, J. A., "Fronts Propagating with Curvature-Dependent Speed: Algorithms Based on Hamilton-Jacobi Formulations," *Computational Physics* **79**, 12–49 (1988).

[17] Zhao, F., Zhang, H., Wahle, A., Scholz, T. D., and Sonka, M., "Automated 4d segmentation of aortic magnetic resonance images," in [*BMVC*], 247–257 (2006).

[18] Kohlberger, T., Cremers, D., Rousson, M., Ramaraj, R., and Funka-Lea, G., "4D Shape Priors for a Level Set Segmentation of the Left Myocardium in SPECT Sequences," in [*MICCAI*], 92–100 (2006).

[19] Abufadel, A., Yezzi, T., and Schafer, R., "4D segmentation of cardiac data using active surfaces with spatiotemporal shape priors," in [*SPIE*], (2007).

[20] Boykov, Y. and Kolmogorov, V., "An experimental comparison of min-cut/max-flow algorithms for energy minimization in vision.," *PAMI* **26**(9), 1124–1137 (2004).

[21] Yu, T., Xu, N., and Ahuja, N., "Reconstructing a Dynamic Surface from Video Sequences Using Graph Cuts in 4D Space-Time," in [*ICPR*], 245–248 (2004).

[22] Li, Y., Sun, J., and Shum, H.-Y., "Video object cut and paste," in [*SIGGRAPH*], 595–600 (2005).

[23] Adams, R. and Bischof, L., "Seeded region growing," *PAMI* **16**(6), 641–647 (1994).

[24] Sinop, A. K. and Grady, L., "Accurate banded graph cut segmentation of thin structures using laplacian pyramids.," in [*MICCAI*], 896–903 (2006).

[25] Shi, J. and Malik, J., "Normalized cuts and image segmentation," *PAMI* **22**(8), 888–905 (2000).